JOURNAL OF GEOPHYSICAL RESEARCH, VOL. 96, NO. B13, PAGES 21,535–21,548, DECEMBER 10, 1991

Penetration of a Quasi-statically Slipping Crack Into a Seismogenic Zone of Heterogeneous Fracture Resistance

HUAJIAN GAO

Division of Applied Mechanics, Stanford University, Stanford, California

JAMES R. RICE

Division of Applied Sciences and Department of Earth and Planetary Science, Harvard University, Cambridge, Massachusetts

JIN LEE

Division of Applied Mechanics, Stanford University, Stanford, California

This paper is concerned with some aspects of nonuniform stressing above a deep creeping portion of a fault zone prior to a large crust-breaking earthquake. The model that we use involves a slipping crack, representing the deeper, more stably sliding portions of the fault zone, which penetrates upward from depth and is blocked in the lower region of the seismogenic zone. When conditions are uniform along strike, the upward penetration at the crack front is by mode III in strike-slip fault zones but by mode II in thrust or normal fault zones. Two major results are reported. First, we analyze approximately, via a linear perturbation formulation, how a tectonic crack front encounters and ultimately shears through arrays of localized "asperities" that are distributed parallel to the crack front and have a toughness which is greater than that of adjoining segments of the fault zone. Using a fast Fourier transform based numerical procedure to simulate crack penetration into asperities, we find a notable difference between mode II and mode III crack fronts in that the former penetrates approximately twice as far between the asperities as the latter under the same loading level. This is interesting because observations of slip distribution in large earthquakes suggest that there is a significant aseismic component to the total slip budget in subduction zone earthquakes, which in contrast does not seem to be present in strike-slip zone earthquakes, and also that the surface slip distribution in continental dip-slip faulting is typically much more irregular than for strike-slip faulting. In a simulation involving multiple rows of periodic asperities we note that the more deeply penetrating mode II crack front contacts more asperities simultaneously while breaking them at different load levels compared to the less flexible mode III crack front, which simply breaks one row of asperities and jumps (unstably) to the next. The second major result concerns whether a straight crack front in the lithosphere along a strike-slip fault zone is configurationally stable, that is, whether the crack front will tend to remain straight as the crack penetrates upward from depth. It is found that for infinitesimal perturbations of the straight front beyond a critical wavelength, of the order of the crustal lithosphere thickness, the stress intensity factor is higher at the most advanced portions of the crack front rather than at the least advanced; the opposite is true at shorter wavelengths. When resistance to crack growth is essentially uniform over the fault plane, this means that the straight crack front is configurationally unstable at long wavelengths. The issue of configurational stability is related to the concept of fault segmentation, which is based on the observation that fault zones, particularly long ones, do not rupture along their entire length during a single earthquake. Effect of a vertical gradient of fracture resistance is discussed in the appendix, where it is shown that a significant upward gradient of resistance to crack growth may completely stabilize the straight crack configuration.

INTRODUCTION

The concept that crustal earthquakes involve the loading of a shallow crustal zone by slip at depth has been adopted by many authors [e.g., *Savage and Burford*, 1973; *Turcotte and Spence*, 1974; *Prescott and Nur*, 1981; *Li and Rice*, 1983; *Tse et al.*, 1985]. There is general agreement that the shallow lithosphere is largely elastic over the time scale of interest, so that the earthquake faulting can sometimes be modeled as a slipping crack in otherwise elastic surroundings. The crack front penetrates upward from depth along the fault zone and is blocked in the lower region of the seismogenic layer. The crack surfaces represent the deeper portions of the fault where the slip motion is accommodated mostly by aseismic shear due to the prevailing temperature and perhaps pore pressure conditions, while the uncracked regions, consisting of cooler crustal rocks, are considered to be locked in a brittle manner; that is, they do not slide at all or do so very little in the form of small earthquakes during all but a few moments of the seismic cycle. If overall plate motion is to occur, the aseismic deformation below concentrates stress onto, and ultimately shears through, the whole locked region. During this process, gradual rupture is promoted along the lower margin of the slip-deficient zone, enabling the upward penetration of the crack front until the loss of equilibrium in the form of a large earthquake. According to the usual terms of crack mechanics the upward penetration at the crack front is by mode III (antiplane shear) in strike-slip fault zones but by mode II (in-plane shear) in thrust or normal fault zones.

Paper number 91JB02261.
0148-0227/91/91JB-02261$05.00

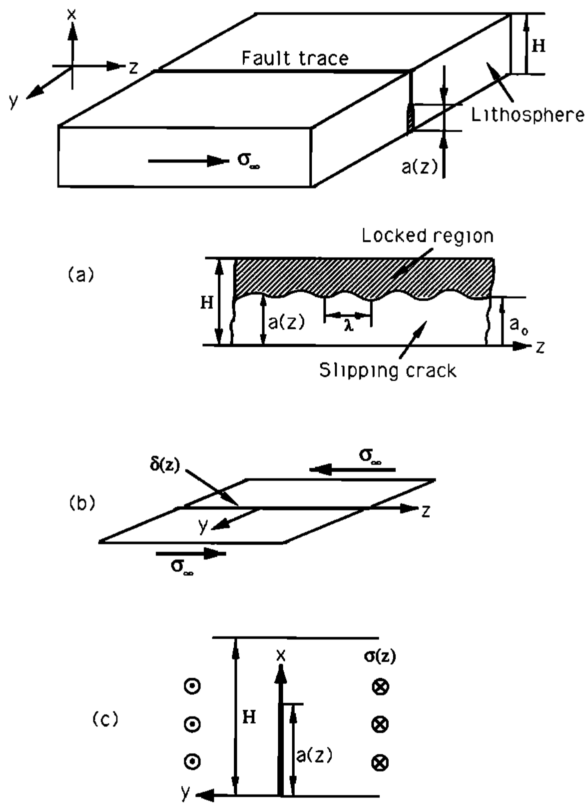

Fig. 1. (*a*) A crack model for stressing in a strike-slip fault zone. The idea of the "line spring": the three-dimensional problem has been reduced to two two-dimensional problems of (*b*) a plane stress deformation in the $y - z$ plane and (*c*) a mode III crack in the $x - y$ plane.

Such an elastic-brittle crack model, which we adopt here, can be interpreted as [e.g., *Rice* 1980] the limiting case of slip-weakening models when the size of the zone over which shear strength degrades is small compared to other relevant dimensions such as the width of the locked seismogenic layer. *Stuart* [1979] and *Stuart and Mavko* [1979] have applied such slip-weakening concepts to crustal instabilities, and in the appropriate limit their models show cracklike penetration of slipping zones into previously nonslipping (or little slipping) zones. In recent years a more elaborate crustal earthquake model has been developed [*Tse and Rice*, 1986], in which the slip and stress distributions on the fault surface are required to satisfy laboratory-constrained rate- and state-dependent friction laws with temperature and normal stress (and hence depth) variation of frictional constitutive parameters. As can be seen from the *Tse and Rice* [1986] strike-slip results and also those of *Stuart* [1988], who adopted a similar description of thrust faulting, the slip distribution histories that result are suggestive of a cracklike upward progression of a slipping region into an effectively locked region throughout most of the earthquake cycle. Thus the crack model which we adopt here, with a fracture criterion to convert locked into slipping material at the crack tip, seems often to provide an acceptable, if highly simplified, description of inhomogeneous fault zone deformation.

The resistance of rocks in the fault zone against fracture (slip) may vary in a nonuniform manner, which deforms the penetrating crack front into a complicated profile. In the model shown in Figure 1*a* for a strike-slip fault, the lithosphere is considered as a linearly elastic isotropic plate of uniform thickness H containing a crack of varying depth $a(z)$ with a typical wavelength λ and an average depth a_0 in response to a heterogeneous strength distribution along the fault. In regions of high thermal gradient, for which the lower crust could be expected to relax in shear on the interearthquake time scale, this lithosphere plate represents the middle and upper crust. In cooler settings it may include part of the upper mantle. Such a plate model with variable crack depth has previously been studied by *Li and Rice* [1983] and *Tse et al.* [1985] using the "line spring" concept originally developed by *Rice and Levy* [1972] for treating part-through cracks in elastic plates. However, as pointed out in those works, the line spring analyses are valid only at sufficiently long wavelengths, requiring λ to be significantly larger than the plate thickness H. This restriction severely limits the validity of the line spring results for short-wavelength applications such as those we shall consider, which concern effects of localized asperities having a slightly higher fracture toughness value than their surrounding regions but having size scales much smaller than the plate thickness. To study the earthquake mechanism, various authors have used the idea of representing the heterogeneous strength distribution in a fault plane by asperities [e.g., *Madariaga*, 1979; *McGarr*, 1981; *Lay et al.*, 1982; *Das and Kostrov*, 1983].

For the localized, short-wavelength effects that we consider it is very costly to implement conventional numerical procedures such as the finite element or boundary element method (BEM). In the recent development of three-dimensional crack mechanics, *Rice* [1985] developed a linear perturbation method for analyzing planar cracks with fronts deviating slightly from some regular geometry such as a straight line or a circle. *Gao and Rice* [1986] subsequently applied the perturbation method to a shear-loaded half plane crack and derived the first-order perturbation solution for the shear stress intensity factors along a slightly curved crack front. The perturbation results will be applied in this paper to analyze approximately how a tectonic shear crack encounters and ultimately shears through an array of asperities that are strung out parallel to the crack front and are much smaller in size than other characteristic length dimensions, such as the depth of the as yet uncracked seismogenic zone. Our numerical simulation reveals a notable difference between mode II and mode III crack fronts in that the former penetrates approximately twice as far between the asperities as the latter under the same loading level. While it lies beyond the scope of our linearized perturbation analysis, we expect that for moderately tough asperities the more deeply penetrating mode II crack front segments will more readily tend to coalesce unstably with one another ahead of the asperities. Therefore the crack front advances and leaves unbroken asperities behind, whereas the less flexible mode III crack front will more likely tend to break the asperities in a seismic manner. This is interesting because observations [e.g., *Scholz*, 1990, p. 317] of the distribution of slip in large earthquakes suggest that there is a significant aseismic component to the total slip budget in subduction zone earthquake cycles, which is not, or has not been perceived to be, present to a comparable degree for strike-slip earthquakes. *Scholz* [1990, p. 157] also compares surface slip distributions in the 1983 Borah Peak and 1979 Imperial Valley earthquakes. He comments that ". . . the surface slip in the dip-slip case (Borah Peak) is much more irregular than in the strike-slip case (Imperial Valley). This observation is fairly typical . . . " (although no systematic comparison based on many examples seems to have been done yet). The differences in seismic behavior may be explained by the different behaviors of mode II and III crack fronts in encountering asperities during earthquake faulting, although differences in fault zone materials, at least when subduction zones are considered, and possibly differences in the uniformity of loading over large distances along strike make direct comparisons difficult.

To provide further insight, a simulation of crack penetration into multiple rows of asperities is presented, which indicates that the more deeply penetrating mode II crack front interacts with more asperities in different rows and breaks them at different loading levels compared to the less flexible mode III front, which, for the geometry of our simulation, simply breaks one row of asperities and jumps (unstably) to the next row. Implications may be that foreshocks in strike-slip fault zones tend to be larger but less frequent prior to a major earthquake compared to those in tectonically similar thrust or normal fault zones. Our present study on the short-wavelength perturbations in crack front complements the previous line spring analysis of *Tse et al.* [1985] on stressing of large-scale locked patches along a strike-slip fault.

Another issue to be addressed in the paper is related to fault segmentation, a concept which is based on the observation that fault zones, particularly long ones, do not rupture along their entire length during a single earthquake. There are increasing geological and seismological indications [e.g., *Schwartz and Coppersmith*, 1984; *Schwartz and Sibson*, 1988] that the location of earthquake rupture is not random, that there are recognizable physical properties of fault zones which control the nucleation point and lateral extent of rupture and divide a fault into segments, that ruptures with the same characteristics often repeat in the same location, and that independent rupture segments can persist through several seismic cycles. It is natural to relate fault segmentation to complex structural or geometrical features of fault zones: Fault traces meander and cross, mechanical properties of faults and their adjoining crust are heterogeneous, and fault loading may be due to erratic tectonic processes.

But some aspects of the segmentation may follow from the intrinsic mechanics of faulting to the extent that they would be maintained even if all complexity in the Earth's structure were eliminated. Such a possibility was demonstrated in a fault model by *Horowitz and Ruina* [1989], which produced complex slip patterns, even with no complexity in geometry or heterogeneity in material properties, at least for choices of rate- and state-dependent frictional properties which put their system rather close to, but on the unstable side of, the neutrally stable state. Suggestions that the dynamics of uniform fault must inevitably lead to spatiotemporally complex slip have been made recently based on inherently discrete fault mechanics by *Bak and Tang* [1989] and *Ito and Matsuzaki* [1990], who use a cellular automata fault model, and by *Carlson and Langer* [1989], who analyze the dynamics of a Burridge-Knopoff array of spring-connected rigid blocks obeying velocity-weakening friction. The issue remains somewhat clouded, however. *Rice* [1991] has noted that unlike the *Horowitz and Ruina* [1989] model, these inherently discrete models have no well-defined continuum limit as the cell or block spacing is reduced toward zero (the models also simplify true elasticity relationships between slip and stress distributions on faults to nearest-cell or nearest-block stress transfers). The *Horowitz and Ruina* [1989] model, like other fault models based on rate- and state-dependent friction [e.g., *Tse and Rice*, 1986; *Stuart*, 1988] or just on simple slip weakening [*Stuart*, 1979; *Stuart and Mavko*, 1979], has such a limit because of the finite characteristic length scale which enters the model, as the critical slip distance for state evolution or for slip weakening. This issue may be critical to the origin of complexity in the inherently discrete models. *Rice* [1991] presented three-dimensional numerical simulations of slip on a vertical fault between elastically deformable continua, using rate- and state-dependent friction. His examples show cases for which spatiotemporally complex slip histories, reminiscent of those of the inherently discrete models, result when the computational grid spacing is too coarse to properly simulate a continuum but for which the complexity disappears, and the response settles down to periodically repeated earthquakes much like the earthquakes in the two-dimensional *Tse and Rice* [1986] study, with slip histories that are essentially identical at each place along strike, as grid spacing is reduced to sizes that reasonably model continuum response. That is, the complexity disappears (at least in *Rice*'s [1991] examples, which do not include the near-neutral-stability cases of *Horowitz and Ruina* [1989]) when each cell of the computational grid is made sufficiently small, so that a single cell is unable to undergo unstable slip without some of its neighbors slipping also (this situation is never attained in the inherently discrete models).

Thus the extent to which fault models that are uniform along strike can produce slip distributions which are not uniform is far from resolved. In this paper we use the simple elastic-brittle crack model to address the issue. In the case of a homogeneous strike-slip fault model, with a fracture toughness that is uniform over all the fault plane, we show that a critical wavelength λ_{cr} exists which is of the order of one to a few times the elastic plate thickness. Above λ_{cr} a straight crack front has the possibility of becoming configurationally unstable even in the absence of any variation in geometry or material properties in the fault plane. Our analysis is based on an asymptotic interpolation between the line spring results of *Tse et al.* [1985] at long wavelengths and the half plane crack perturbation results of *Gao and Rice* [1986] at short wavelengths. An approximate first-order formula is constructed for calculating the stress intensity factor along a perturbed crack front at all wavelengths; the interpolation is shown to be consistent with some three-dimensional finite element results. At wavelengths larger than λ_{cr} the stress intensity factor is greater at the most advanced, rather than the least advanced, portions of the wavy crack front; the opposite is true at wavelengths shorter than λ_{cr}. However, the spatial variation of fracture toughness also plays a key role in the configurational stability analysis, and we show in the appendix that introduction of a positive upward gradient in fracture resistance can cause configurational stability to be retained at wavelengths far beyond λ_{cr}.

BACKGROUND

In studying the faulting processes with a perturbed crack front in a lithospheric plate one may use a half plane crack in an infinite solid to model problems at short wavelengths and

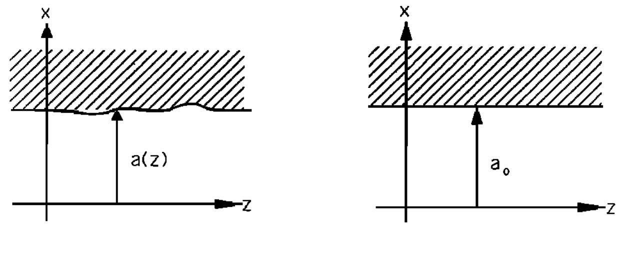

Fig. 2. (*a*) A half plane crack with a slightly curved crack front. (*b*) The reference straight crack front.

use the line spring model at sufficiently long wavelengths. For convenience, we briefly review the basic perturbation and line spring equations below.

Perturbation Solutions for a Half Plane Crack

Consider a shear loaded half plane crack on the plane $y = 0$ with a slightly curved crack front along the arc $\{x = a(z), y = 0\}$ in an infinite solid (Figure 2*a*). Assume that the stress concentration at the crack tip is measured by shear stress intensity factors $K_\alpha^0[a_0]$ (α = II, III) when the crack front lies along a reference straight line $x = a_0$ parallel to the z axis (Figure 2*b*). For the perturbed crack front, *Gao and Rice* [1986] have derived

$$K_{\mathrm{II}}(z) = K_{\mathrm{II}}^0[a(z)]\left\{1 + \frac{1}{2\pi}\frac{2-3\nu}{2-\nu} \cdot \mathrm{PV}\int_{-\infty}^{+\infty}\frac{da(z')/dz'}{z'-z}\,dz'\right\} - \frac{2}{2-\nu}K_{\mathrm{III}}^0[a(z)]\frac{da(z)}{dz} \qquad (1a)$$

$$K_{\mathrm{III}}(z) = K_{\mathrm{III}}^0[a(z)]\left\{1 + \frac{1}{2\pi}\frac{2+\nu}{2-\nu} \cdot \mathrm{PV}\int_{-\infty}^{+\infty}\frac{da(z')/dz'}{z'-z}\,dz'\right\} + \frac{2(1-\nu)}{2-\nu}K_{\mathrm{II}}^0[a(z)]\frac{da(z)}{dz} \qquad (1b)$$

to the first-order accuracy in the deviation of $a(z)$ from constancy. Here PV denotes principal value in the Cauchy sense, and ν is the Poisson ratio. In writing (1) for any given z, we have chosen a reference straight crack front along $x = a(z)$.

It is commonly assumed that fracture processes are controlled by the energy release rate

$$G = \frac{(1-\nu)(K_{\mathrm{II}})^2 + (K_{\mathrm{III}})^2}{2\mu} \qquad (2)$$

(μ is shear modulus) at the crack front or controlled by the maximum shear stress intensity factor

$$K = (K_{\mathrm{II}}^2 + K_{\mathrm{III}}^2)^{1/2} \qquad (3)$$

That is, cracks grow only when G or K reaches a critical value. For a strike-slip fault the stress concentration at the straight crack front is by mode III only, but when the front is perturbed to the curved position $x = a(z)$, a mode II intensity factor $K_{\mathrm{II}}(z)$ of first order of magnitude will be induced according to (1), giving a second-order contribution to the control parameters G or K. Similarly, for thrust or normal faults where mode II dominates, it may be shown that K_{III} appears as second-order small quantities in G or K. Therefore for these special cases treated in the present first-order analysis the coupling effect between the shear modes can be ignored so that the perturbation equations (1) are rewritten as

$$K(z) = K^0[a(z)]\left\{1 + \frac{M_\alpha}{2\pi}\mathrm{PV}\int_{-\infty}^{+\infty}\frac{da(z')/dz'}{z'-z}\,dz'\right\} \qquad (4)$$

for all crack modes, where the constant coefficients M_α are

$$M_{\mathrm{I}} = 1 \qquad M_{\mathrm{II}} = (2-3\nu)/(2-\nu) \qquad M_{\mathrm{III}} = (2+\nu)/(2-\nu) \qquad (5)$$

For completeness, we have included the mode I perturbation result so that (4) and (5) correspond to a tensile crack when α = I, a strike-slip fault when α = III, and a thrust or normal fault when α = II.

Line Spring Model

The idea of the line spring model is to reduce the complicated three-dimensional crack problem shown in Figure 1*a* into two two-dimensional plane problems shown in Figures 1*b* and 1*c*. The lithosphere is represented as a two-dimensional elastic plane containing a line of slip discontinuity along the z axis representing the fault trace (Figure 1*b*). Using dislocation theory, it may be shown that the thickness averaged shear stress $\sigma(z)$ is related to the thickness-averaged slip $\delta(z)$ along $y = 0$ by [e.g., *Li and Rice*, 1983]

$$\sigma(z) = \sigma_\infty - \frac{\mu(1+\nu)}{2\pi}\int_{-\infty}^{\infty}\frac{1}{z-z'}\frac{\partial\delta(z')}{\partial z'}\,dz' \qquad (6)$$

where the integral term represents the contribution due to the slip dislocation distribution $\delta(z)$. On the other hand, the slip $\delta(z)$ at a chosen position z is regarded as being induced by the local stress $\sigma(z)$ according to the two-dimensional mode III crack in Figure 1*c* with crack depth taken as the local value $a(z)$.

For a two-dimensional mode III crack with a straight crack front at $x = a$ subjected to a remote stress σ_∞, the stress intensity factor has the known solution [*Tada et al.*, 1985]

$$K^0[a] = \sigma_\infty[2H\tan(\pi a/2H)]^{1/2} \qquad (7)$$

The thickness averaged slip δ is related to σ_∞ by

$$\delta = \sigma_\infty/k \qquad (8)$$

where the stiffness k can be derived from the compliance relation

$$\frac{\partial}{\partial a}\left[\frac{1}{2}\left(\frac{1}{kH}\right)(\sigma_\infty H)^2\right] = \frac{(K^0[a])^2}{2\mu} \tag{9}$$

following the definition of the energy release rate (on the right side) as the decrease in the total potential energy (within the brackets) per unit crack extension. Substituting (7) into (9), noting that $1/k = 0$ when $a = 0$, and integrating both sides of (9) with respect to the crack depth parameter a, one obtains [*Li and Rice*, 1987]

$$\frac{1}{k(a)} = \frac{4H}{\pi\mu} \ln\left[\frac{1}{\cos(\pi a/2H)}\right] \tag{10}$$

It is assumed in the line spring model that $\delta(z)$ and $\sigma(z)$ in (6) are related by

$$\delta(z) = \sigma(z)/k[a(z)] \tag{11}$$

where $k[a(z)]$ is taken to be the two-dimensional solution (10) with the argument a replaced by the local crack depth $a(z)$. Solving the coupled equations (6) and (11) for $\sigma(z)$ and $\delta(z)$, the stress intensity factor along the curved crack front is given by

$$K(z) = \sigma(z)\{2H \tan[\pi a(z)/2H]\}^{1/2} \tag{12}$$

BREAKING OF LOCALIZED ASPERITIES ALONG A CREEPING FAULT

Consider a shear crack representing a slipping fault zone at depth which penetrates into arrays of asperities in the seismogenic layer. Assume that the asperity size is much smaller than other relevant tectonic length dimensions so that the half plane crack formula (4) can be applied to the perturbations caused by those asperities.

First observe that other than the coefficient M_α the shear mode perturbation formulae shown in (4) and (5) are completely analogous to that of the tensile mode I crack. An analogy is then established between the process of a slipping crack penetrating asperities and that of the "crack trapping" in which a mode I crack advances nonuniformly in a composite material with crack front segments trapped by contact with the second phase tough inclusions whose fracture toughness exceeds the local stress intensity. This process has been identified as one of the important toughening mechanisms for materials in engineering applications. In an earlier study on crack trapping, *Gao and Rice* [1989] used the mode I perturbation formula and devised a fast Fourier transform (FFT) numerical procedure for simulating crack penetration into periodical arrays of blocking particles. We shall use the same procedure to simulate the penetration of a shear crack into periodic arrays of asperities in a fault plane.

For convenience, the numerical procedure of *Gao and Rice* [1989] is reviewed in a form suitable for the present application. Assume that the fracture toughness varies in the fault plane by a function $K_c = K_c(x, z)$. The slipping crack will grow at positions along the crack front where the stress intensity factor $K(z)$ exceeds the local toughness K_c. To simulate the crack penetration process, it is convenient to use the following "viscoplastic" crack growth model

$$\begin{aligned} &\partial a(z,t)/\partial t = \rho[K(z,t) - K_c(a(z,t), z)] \quad && K > K_c \\ &\partial a(z,t)/\partial t = 0 && \text{otherwise} \end{aligned} \tag{13}$$

where t is a "time" parameter and ρ represents the "viscosity" of the system. By making ρ sufficiently large or else (as we do) by waiting sufficiently long for a new equilibrium configuration of the crack front to be approached after each small increase of load, we can make (stable) crack growth occur arbitrarily close to the condition that $K = K_c$ everywhere along the crack front during growth.

The local stress intensity $K = K(z, t)$ is related to $a(z, t)$ by the perturbation relation (4) at a given time t. In principle, one can solve the coupled equations (4) and (13) for $K(z, t)$ and $a(z, t)$. The final equilibrium profile corresponds to $a(z) = a(z, \infty)$ after each step increase of the load. While it is often impossible to solve these coupled equations analytically, numerical procedures can be designed by discretizing the governing equations into small time steps and then updating $a(z, t)$ and $K(z, t)$ according to (4) and (13) for each step. The time step Δt for any given value of ρ can be adjusted to achieve the optimum rate of numerical convergence.

We apply the above simulation procedure to crack penetration of periodic arrays of asperities with center-to-center spacing of $2L$. The asperities have a fracture toughness $\hat{K}_c$ which is twice the toughness K_c of their surrounding regions. Also, assume a crack length a and a shear load σ in the effective sense so that the stress intensity factor for a straight front can be written in the form

$$K^0[a] = f\sigma(a)^{1/2} \tag{14}$$

f being a geometric constant independent of a and σ. Before the penetration starts, the crack front lies along a straight line at $x = a_i$, and crack growth is imminent at a load level that meets the condition $f\sigma(a_i)^{1/2} = K_c$. With further increase of the load the crack front will grow into a new equilibrium state having a slightly curved profile. Let $a(z, t)$ and $K(z, t)$ be expanded into Fourier series,

$$\begin{aligned} a(z,t) &= \mathrm{Re}\left[\sum_{n=-\infty}^{\infty} A_n e^{in\pi z/L}\right] \\ K(z,t) &= \mathrm{Re}\left[\sum_{n=-\infty}^{\infty} K_n e^{in\pi z/L}\right] \end{aligned} \tag{15}$$

Substituting (15) into (4) and carrying out the principal value integrations, one may show that the Fourier coefficients A_n and K_n are related by [*Gao and Rice*, 1986]

$$\begin{aligned} K_0 &= K^0[A_0] = f\sigma(A_0)^{1/2} \\ K_n &= \left\{\frac{dK^0[A_0]}{dA_0} - \frac{n\pi M_\alpha}{2L} K^0[A_0]\right\} A_n \\ &= \frac{K_0}{2}\left\{\frac{1}{A_0} - \frac{n\pi M_\alpha}{L}\right\} A_n \end{aligned} \tag{16}$$

These relations are valid only for small perturbations, i.e., when L/A_0 and $|A_n|/A_0 \ll 1$.

Using the FFT method to carry out the expansion and inversion of the Fourier series in (15), one may devise the following iteration procedure for simulating the process of the crack penetration into asperities: At a load level σ of interest the initial crack front profile $a(z, 0)$ (taken as a

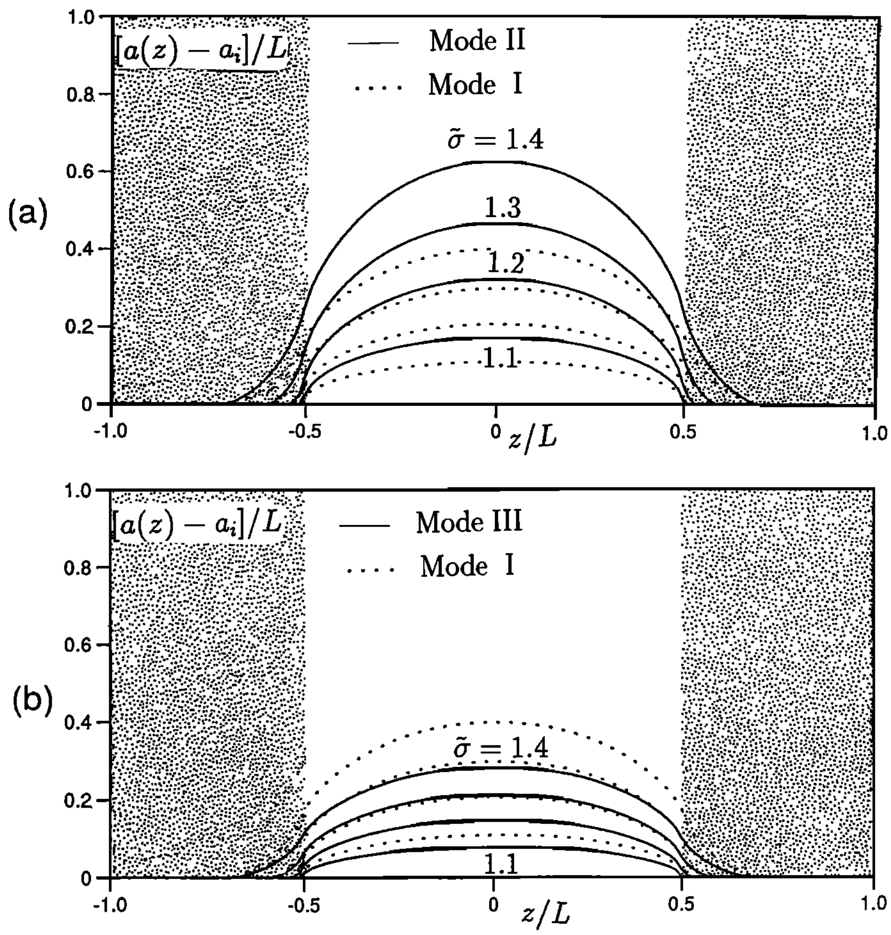

Fig. 3. A crack penetrating a periodic array of straight-edged asperities with $\hat{K}_c/K_c = 2$: (*a*) mode I and II and (*b*) mode I and III.

constant at the start of the procedure) is expanded into a Fourier series via a FFT expansion, and the coefficients K_n in the second equation of (15) are calculated from the perturbation equations (16). A FFT inversion by (15) gives the distribution of $K(z, 0)$. Equation (13) is then used, for a chosen time interval Δt and constant ρ, to calculate the amount of growth $\Delta a(z, 0)$ for one period $-L < z < L$, therefore updating $a(z, \Delta t)$ as $a(z, 0) + \Delta a(z, 0)$. The above procedure is repeated to calculate the subsequent growth until the final equilibrium state is achieved in which $a(z, t)$ no longer increases by any substantial amount (e.g., less than $10^{-6}L$), indicating that the conditions $K(z) = K_c$ and $K(z) = \hat{K}_c$ are satisfied to the accuracy required along the corresponding portions of the crack front. Then the load σ may be increased by another step and the same sequence of steps followed. The above procedure can be made rapidly convergent if the time steps are properly chosen (scaling inversely with the arbitrarily chosen constant ρ).

Figure 3 depicts the crack front penetration profiles in one period $-1 < z/L < 1$ for a periodic array of asperities having flat edges. The asperities are spaced at $2L$ with a gap L between them and aligned parallel to the z axis so that the crack front encounters them simultaneously. The initial crack length a_i is taken to be 10 times L (a_i ought to be large compared to L, since this is based on a half plane crack analysis) with

$$f\sigma_i(a_i)^{1/2} = K_c \tag{17}$$

A nondimensional load parameter defined as $\tilde{\sigma} = \sigma/\sigma_i$ is used to indicate the global level of the tectonic stressing. The fracture toughness $\hat{K}_c$ of the asperities is taken as twice the value of K_c. As the load parameter $\tilde{\sigma}$ is increased with a step increment of 0.1, equilibrium profiles of a mode II crack front are shown as solid lines in Figure 3*a*, while those of a mode III crack front are shown similarly in Figure 3*b*. The mode I crack trapping profiles computed by *Gao and Rice* [1989] are shown as dotted lines for comparison. The results indicate that the mode II crack front penetrates approximately twice as far between the asperities as the mode III crack fronts under the same loading level. A mode I crack front appears to be more flexible than a mode III front but less so than a mode II front. At the present toughness ratio $\hat{K}_c/K_c = 2$ the full penetration of the asperities occurs when $\tilde{\sigma}$ reaches 1.5.

Rigorously, the penetration curves in Figure 3 as predicted from the linearized perturbation theory are correct only to the first-order accuracy in the crack front deviation from a straight line. Recently, *Fares* [1989] has performed a BEM analysis of the crack trapping and showed that for a mode I crack front blocked by sufficiently tough particles, there is a maximum local stress intensity factor $K(z) = WK_c$, which can be generated at the crack front prior to final instability.

If the toughness ratio $\hat{K}_c/K_c$ is less than W, the crack front will eventually break through the blocking particles. But if the toughness ratio is more than W, the penetrating crack front segments will tend to coalesce unstably with one another ahead of the particles so that the crack front bypasses the still intact particles, causing the so-called "crack bridging" process which has been identified as another important toughening mechanism of a brittle matrix by inclusions [e.g., *Krstic*, 1983]. Similar phenomena are expected to exist for shear crack penetration into asperities. While it lies beyond the scope of our linearized perturbation analysis, we expect that for moderately tough asperities the more deeply penetrating mode II crack front segments will more readily tend to coalesce with one another, so that the crack front advances and leaves unbroken asperities behind, whereas the mode III crack front will require a significantly higher asperity toughness to do so. For a mode I crack front the transition from particle breaking to particle bridging is found to occur at $W = 3.52$ for round particles spaced by two diameters. On the basis of the perturbation analysis for all three modes we expect a lower ratio at transition in mode II and higher in mode III. Further work for the mode I case, which goes beyond first-order perturbations, has also been reported by *Bower and Ortiz* [1990], who fully developed a technique of successive perturbations suggested by *Rice* [1989] and applied it, among other cases, to crack growth around obstacles.

In the asperity models of *Lay and Kanamori* [1981] and *Lay et al.* [1982] for subduction zone earthquakes, asperities representing highly stressed regions are assumed to be fully coupled to seismic activities while less stressed regions normally slip aseismically but may be ruptured in response to rupture of the asperities. *Scholz* [1990] pointed out that the aseismically slipping regions in subduction zones should be further divided into two categories, namely, those that slip aseismically but may be ruptured in response to rupture of the asperities and those that always slip aseismically and do not rupture in response to rupture of adjoining regions. Analogously, our crack model also involves two distinctly different regions: asperities with higher fracture toughness which rupture seismically and the rest of the surroundings with much lower slip resistance, representing largely aseismic slipping regions. In the faulting process, tough asperities may be left intact (unbroken) as the slipping zone advances and coalesces ahead of them. The regions surrounding asperities are thus also divided into two categories: the penetrated regions which always slip aseismically and the as yet unpenetrated regions which may be ruptured in response to rupture of asperities.

The interesting result that mode II crack fronts are more flexible than mode III crack fronts does seem to be consistent with differences in seismic coupling in strike-slip and subduction zone environments. *Scholz* [1990, p. 317] reviewed observations of the distribution of slip in large earthquakes and stated that " . . . aseismic slip is a rare phenonmenon in faulting in continental crust. . . . However, a lack of complete seismic coupling seems to be common in subduction zones, ..." Due to the "rigidity" of mode III crack front segments, the aseismic slip component in strike-slip zone earthquakes would be much smaller compared to that in subduction zone earthquakes, at least if all other features of the fault interface were (as they are unlikely to be) closely similar in the two situations.

An interesting connection can be made between the above behavior of a crack front and that of a crystal dislocation loop. To see this connection, first consider a closed dislocation loop in an elastic solid. It is well known that the edge portions of the dislocation have higher line tension (self-energy) than the screw portions, so that the equilibrium shape of the loop will be approximately an ellipse with its major axis parallel to the Burgers vector [e.g., *Nabarro*, 1967, pp. 86–87]. In that configuration the edge portion of the loop would appear to be more flexible than the screw portion. *Gao* [1988] made a perturbation analysis of a nearly circular shear mode crack and found that the equilibrium shape of the crack is also approximately an ellipse with the major axis parallel to the direction of the applied shear stress. In that case, the mode II portion of the crack front deforms more (with larger curvature) and thus is more flexible than the mode III portion of the crack front. Similarly, it is easily seen that the difference in line tension between edge and screw dislocation segments would lead to the conclusion that an edge dislocation line will tend to bow out deeper between two pinning points (as in the Frank-Read process) than a screw dislocation under the same level of applied shear stresses [e.g., *Mitchell and Smialek*]. Clearly, this is in qualitative agreement with the behavior of shear mode crack fronts shown in Figure 3.

Figure 4 shows a simulation of the shear crack fronts penetrating multiple arrays of circular shaped asperities (with radius taken as $0.1L$ and toughness ratio as 2). Three rows of asperities are displayed, and each row contains one more asperity so that the penetrating crack front encounters a stronger resistance as it advances upward into the seismogenic layer. Compared to the mode III crack front, the more flexible mode II front interacts with more asperities in different rows. As the crack front penetrates into the first row, part of the front also contacts asperities in the second row, and the interaction effect increases the overall resistance against penetration. The final breakthrough occurs at $\bar{\sigma} = 1.30$. The mode II front interacts with more asperities and breaks through them in multiple unstable events of limited extent and at different load levels, while the less flexible mode III crack front tends to break simultaneously one row of asperities and then to jump (unstably) to the next row. Note that in the simulation we have assumed that the asperities share the same fracture toughness. This assumption may not be generally valid, but to the extent that it may be a good approximation in some cases and the breaking of asperities is recorded in the form of foreshocks prior to a major earthquake, the above observation implies that for comparable stressing environments the foreshocks occurring in strike-slip fault zones would tend to be less frequent but of larger magnitude when they do occur when compared to those in thrust or normal fault zones of similar fault zone properties.

CONFIGURATIONAL STABILITY OF A HOMOGENEOUS STRIKE-SLIP FAULT ZONE

In the previous section we discussed one aspect of the nonuniform stressing in a creeping fault on a sufficiently short-wavelength scale by considering penetration of a continuously slipping zone into localized asperities having a much smaller dimension than overall length scales of the seismogenic layer. If the toughness distributions had been

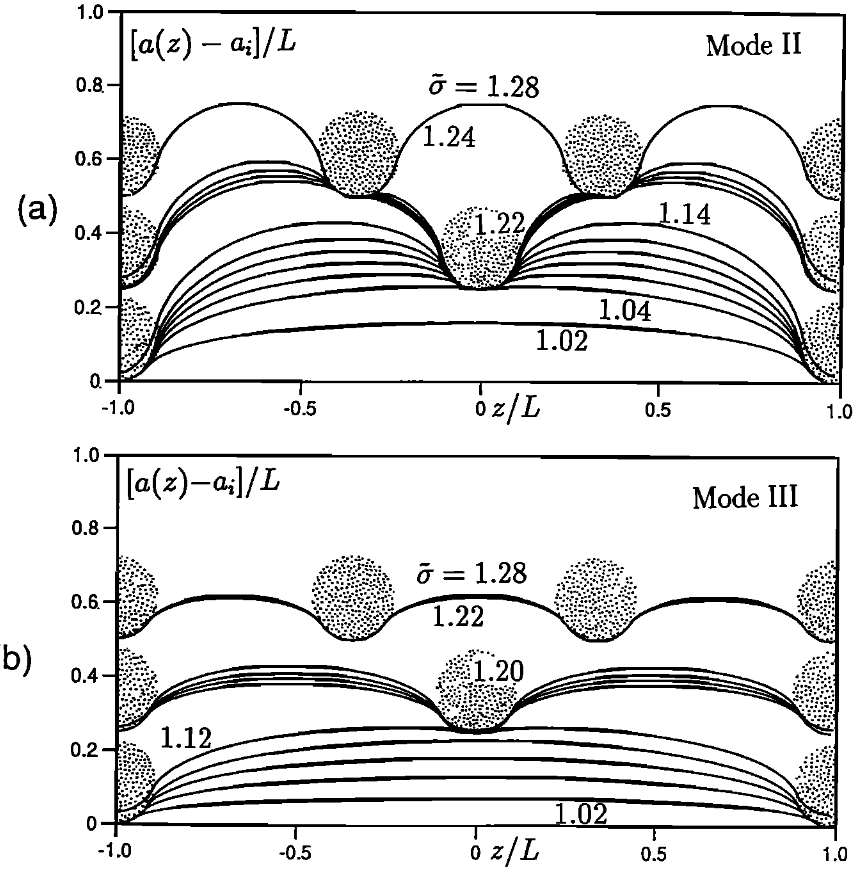

Fig. 4. Profiles of a crack penetrating three rows of round asperities ($\hat{K}_c/K_c = 2$) as the load $\bar{\sigma}$ is increased from 1.0 to 1.3 on a step 0.02: (*a*) mode II and (*b*) mode III.

nearly uniform along strike, the crack fronts would have advanced upward as nearly straight lines, suggesting that a crack front is configurationally stable with respect to short-wavelength perturbations [*Rice*, 1985; *Gao and Rice*, 1986]. However, we show below that a straight crack front configuration is intrinsically unstable for perturbations of sufficiently long wavelength in the absence of any heterogeneous toughness distribution on the fault plane. Also, we hasten to point out that the variation of fracture strength significantly influences the stability analysis. For example, we show in the appendix that the straight crack configuration can be stabilized at long wavelengths when there is a toughness distribution that is uniform along strike but has a significant, positive vertical gradient.

Perturbation Analysis and Configurational Stability

For a straight mode III crack front along a strike-slip fault trace, consider the following cosine wave perturbation (as in Figure 1*a*):

$$a(z) = a_0 + A \cos(2\pi z/\lambda) \tag{18}$$

where A is assumed to be small compared to any other relevant length dimension. For the short-wavelength regime, when $\lambda \ll a_0$, $\lambda \ll H - a_0$, the model of a half plane crack in an infinite solid applies, and substituting (18) into (4) gives [*Gao and Rice*, 1986]

$$K(z) = K^0[a_0] + \left(\frac{dK^0[a_0]}{da_0} - \frac{(2+\nu)\pi}{(2-\nu)\lambda} K^0[a_0]\right) A \cos(2\pi z/\lambda) \tag{19}$$

where the expression for $K^0[a_0]$ has been given by (7). On the other hand, for the long-wavelength regime when $\lambda \gg a_0$, $\lambda \gg H - a_0$, the approximate line spring model applies and substituting first-order expansions

$$\sigma(z) = \sigma_\infty + \sigma_A \cos(2\pi z/\lambda)$$

$$\delta(z) = \sigma_\infty/k(a_0) + \delta_A \cos(2\pi z/\lambda) \tag{20}$$

$$k[a(z)] = k(a_0) + k'(a_0) A \cos(2\pi z/\lambda)$$

into the governing line spring equations (6), (10), and (11), one may derive

$$\frac{\sigma_A}{\sigma_\infty} = \frac{[2\pi(1+\nu)A/\lambda] \tan(\pi a_0/2H)}{1 + 4(1+\nu)(H/\lambda) \ln[1/\cos(\pi a_0/2H)]} \tag{21}$$

The stress intensity factor along the perturbed crack front is then given by

$$K = \sigma(z)\left(2H \tan \frac{\pi a(z)}{2H}\right)^{1/2} = K^0[a_0] + \left(\frac{dK^0[a_0]}{da_0} - \frac{\sigma_A}{A\sigma_\infty} K^0[a_0]\right) A \cos (2\pi z/\lambda) \qquad (22)$$

Combining (19) and (22), we find that $K(z)$ can be generally written as

$$K(z) = K^0[a_0] + \left(\frac{dK^0[a_0]}{da_0} - \frac{C}{\lambda} K^0[a_0]\right) A \cos (2\pi z/\lambda) \qquad (23)$$

where the coefficient $C = C(a_0, \lambda)$ takes the value

$$C = \frac{2\pi(1+\nu) \tan (\pi a_0/2H)}{1 + 4(1+\nu)(H/\lambda) \ln [1/\cos (\pi a_0/2H)]} \qquad (24)$$

at long wavelengths and

$$C = (2+\nu)\pi/(2-\nu) \qquad (25)$$

at short wavelengths.

Assuming that fracture toughness properties are uniform on the fault plane and that the crack growth rate is an increasing function of K, then the amplitude of the cosine perturbation (18) will grow if the maxima of $K(z)$ and $a(z)$ are in phase but decay if they are out of phase. Thus according to (23), disturbances of wavelength λ will decay in amplitude during crack growth if

$$dK^0[a_0]/da_0 < (C/\lambda)K^0[a_0] \qquad (26)$$

and in this case the straight crack front is said to be configurationally stable. Apparently, the stability condition (26) is met only for sufficiently small λ since according to (7)

$$dK^0[a_0]/da_0 = \pi K^0[a_0]/2H \sin (\pi a_0/H) > 0 \qquad (27)$$

If the stability condition (26) is violated, which is the case for sufficiently large λ, then a small perturbation will be enlarged during crack growth so that a straight crack front becomes configurationally unstable. The critical condition is reached when

$$\frac{dK^0[a_0]}{da_0} = \frac{C(a_0, \lambda_{cr})}{\lambda_{cr}} K^0[a_0] \qquad (28a)$$

or

$$\frac{\lambda_{cr}}{C(a_0, \lambda_{cr})} = \frac{2H}{\pi} \sin\left(\frac{\pi a_0}{H}\right) \qquad (28b)$$

The line spring expression (24) predicts a critical wavelength

$$\lambda_{cr} = 4(1+\nu)H\{2 \sin^2 (\pi a_0/2H) - \ln [1/\cos (\pi a_0/2H)]\} \qquad (29)$$

while the short-wavelength expression (25) predicts

$$\lambda_{cr} = [2(2+\nu)H/(2-\nu)] \sin (\pi a_0/H) \qquad (30)$$

(which is out of the range of validity of the half plane crack model, since λ is then comparable to one or both of a_0 and $H - a_0$). These approximate results for λ_{cr} are plotted in Figure 5a in comparison with three-dimensional finite element results to be described shortly. Although our conclusions on configurational stability have to be modified when the fracture toughness varies in the fault plane, as discussed in the appendix for the case of an upward toughness gradient, λ_{cr} remains of interest since it marks the transition of perturbations of a and K from being in-phase to out-of-phase with one another.

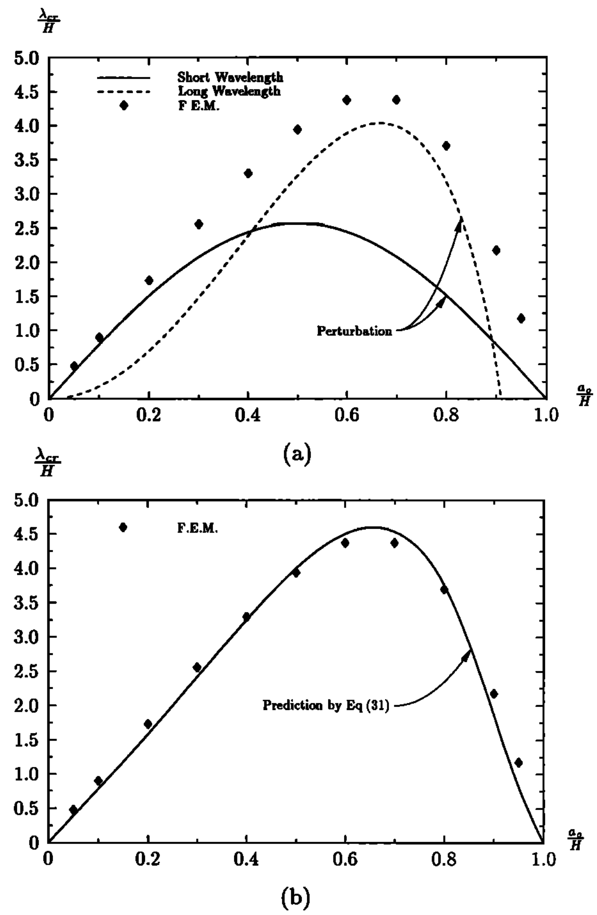

Fig. 5. The critical wavelength in perturbations of a straight mode III crack front along a strike-slip fault: (a) perturbation solutions versus FEM result; (b) prediction from equation (31) versus FEM result.

Finite Element Calculation

To examine the perturbation results for λ_{cr} in the intermediate regime, where neither of the simple limiting case models above applies, we have performed a complete three-dimensional finite element method (FEM) calculation for the perturbed cosine crack front to determine the exact values (within the FEM precision) of λ_{cr}/H as a function of a_0/H.

The FEM mesh layout is shown in Figure 6a. The symmetry of the periodic crack front profile permits us to consider only one-quarter of the body within one period $0 < z < \lambda$ by imposing the symmetry conditions ($u_x = 0$, $u_z = 0$) along the uncracked region in the fault plane $y = 0$ and ($u_x = 0$, $u_y = 0$) along the $x - y$ section planes at $z = 0$ and $z = \lambda/2$. We use the 27-noded isoparametric Lagrangian element (eight nodes at vertices, 12 at midsides, six at face centers, and one at the body center; see Figure 6b) for the general mesh and the collapsed quarter-point singular ele-

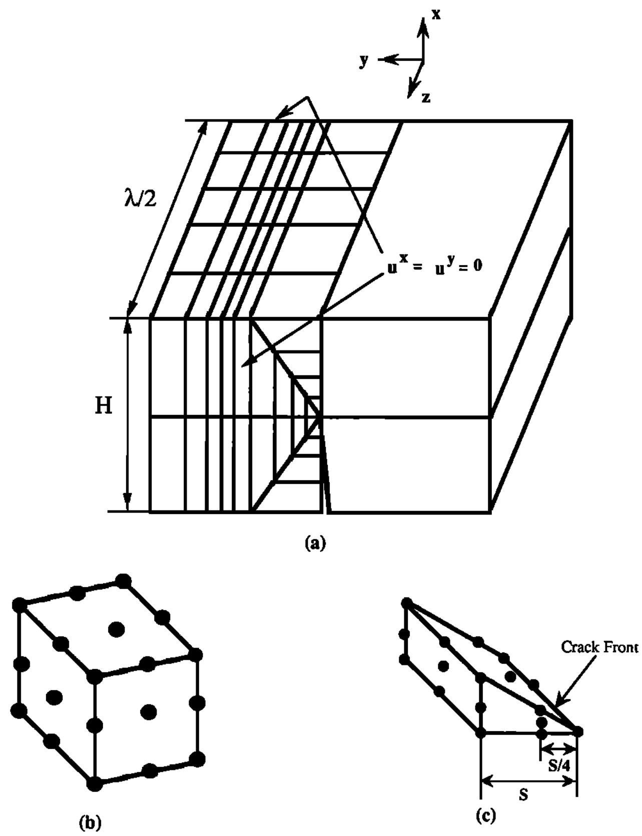

Fig. 6. (*a*) The FEM mesh layout in the half period $0 < z < \lambda/2$ along the periodic wavy crack front. (*b*) The 27-noded element. (*c*) Quarter-point crack-tip element.

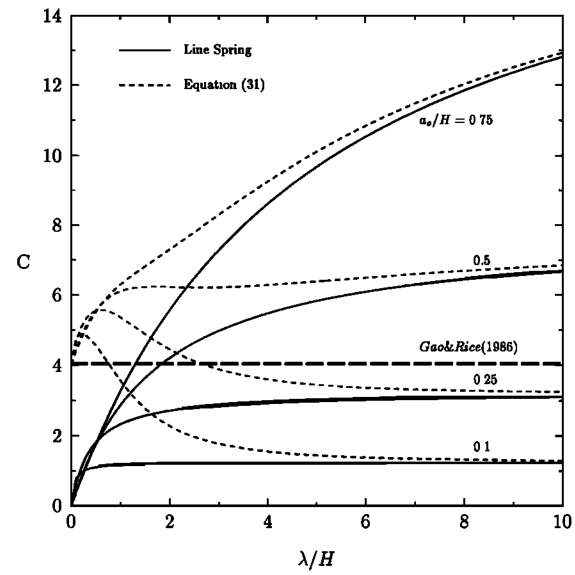

Fig. 7. The coefficient C appearing in equation (23): approximation (31) versus asymptotic expressions (24) and (25).

ment (Figure 6*c*) at the crack tip. The three-dimensional mesh is constructed from a two-dimensional layout in the $x - y$ plane by copying the same mesh over different $x - y$ section planes along the z direction. Nodal positions on elements near the crack tip region are then slightly perturbed in the x direction following the cosine wave crack front profile. The FEM results are further improved by including "transition elements" [*Lynn and Ingraffea*, 1978] outside the crack tip singular element layer. Within the capacity of the convex computer that we use, a maximum of 220 elements are taken which leads to a total three-dimensional mesh of 2211 nodes with 3 degrees of freedom per node. To test our FEM mesh, we first considered the two-dimensional antiplane strain case of a straight mode III crack front and calculated the stress intensity factor by directly matching the asymptotic displacement variation at the crack tip and also by the virtual crack extension method (i.e., local J-integral method; see, for example, *Parks* [1978]). The result based on the direct displacement method shows about 1% error compared with the analytic solution given in (7), while the result predicted from the virtual crack extension method is accurate to within 0.1%.

For a perturbed crack front, both the displacement method and the virtual crack extension method show consistent prediction for the critical wavelength λ_{cr}, with data displayed in Figure 5*a* for 10 different ratios of a_0/H. It is noted that even at the maximum value of λ_{cr}/H around 4.5, the FEM result still shows about 10% difference compared to the line spring prediction. This seems somewhat inconsistent with previous reports (e.g., see results cited by *Parks et al.* [1981] and *Delale and Erdogan* [1982]) that for part-through elliptical tensile cracks in plates the line spring model agrees well with the FEM calculations when the surface length of the crack is of the same order as the crack depth. By varying the perturbation amplitude A and increasing the number of elements dramatically, both near the crack tip region and along the global plate dimensions, we have not found any change in our numerical values for λ_{cr}. This small difference between the mode III FEM and line spring results may reflect the neglect of plate bending (in addition to plane stress) deformation fields in the mode III line spring model as formulated. Such bending effects were included in the mode I line spring model [*Rice and Levy*, 1972]. The variable depth of our mode III crack implies (in the language of plate bending theory) a variable "twisting moment" along the plate edge, and the numerical discrepancy at large λ may be due to its neglect in the line spring model.

An Approximate Perturbation Formula Valid for All Wavelengths

On the basis of the perturbation results at long and short wavelengths as well as the FEM calculation, we may construct an approximate expression for the coefficient C which appears in the K expression (23). One simple expression that matches the asymptotic behaviors (24) and (25) and approximately fits the FEM result for λ_{cr} is

$$C(a_0, \lambda) = \frac{(2+\nu)\pi}{2-\nu} \frac{1}{1+\lambda^2/[16a_0(H-a_0)]} + \frac{2\pi(1+\nu)\tan(\pi a_0/2H)}{1+4(1+\nu)(H/\lambda)\ln[1/\cos(\pi a_0/2H)]} \tag{31}$$

The λ_{cr}/H predicted from the above C approximation is compared with the corresponding FEM result in Figure 5*b*. We also plot (31) with the associated asymptotic expressions (24) and (25) in Figure 7.

On the basis of the C approximation (31) for all wavelengths and the K expression (23), the previous FFT method may be directly extended to study a perturbed mode III crack front in response to a periodic toughness variation in the fault plane with period equal to $2L$ of the same order as the lithosphere thickness. The same steps as summarized from (13) to (17) can be followed after replacing (14) with

$$K_0 = K^0[A_0] = \sigma_\infty[2H \tan(\pi A_0/2H)]^{1/2}$$
$$K_n = \left[\frac{dK^0[A_0]}{dA_0} - \frac{nC(A_0, 2L/n)}{2L} K^0[A_0]\right]A_n \qquad (32)$$

We leave such investigations to future work.

Discussion and Conclusions

In this paper some aspects of the nonuniform stressing along a creeping fault are studied based on a model which represents the slipping portions of a fault as a shear crack penetrating upward into the more brittle seismogenic layer. Two major results are reported. First, we have analyzed approximately, via a first-order perturbation formulation, how a crack front encounters and shears through periodic arrays of localized asperities of slightly higher fracture resistance than their adjoining segments of the fault plane. The configuration of a shear crack, as it gradually penetrates into the asperities at increasing tectonic stress levels, is calculated by equating the local stress intensity factor to the local fracture toughness at every point along the crack front. We find notable differences between mode II and mode III crack fronts in that the former penetrates approximately twice as far between the asperities as the latter under the same loading level. Observations [e.g., *Scholz*, 1990] of the distribution of slip in large earthquakes suggest that there is a significant aseismic component to the total slip budget in subduction zone earthquakes, which, in contrast, does not seem to be present in strike-slip earthquakes and suggest also that continental dip-slip earthquakes have surface slip distributions which are typically much more nonuniform along strike than for comparable size strike-slip earthquakes. Our analysis thus presents one possible physical mechanism for such differences in seismic behavior. The simulation of crack penetration into a multiple arrays of asperities, modeling the increasing fracture resistance at more inner regions of the seismogenic layer, shows that the mode II crack front interacts with more asperities simultaneously and breaks them at different loading levels compared to the less flexible mode III crack front which simply breaks one row of asperities and jumps (unstably) to the next row. To the extent that such a periodic asperity setting provides an approximate description of faulting, this fundamental difference between mode II and III cracks may indicate that foreshocks in strike-slip fault zones tend to be larger but less frequent prior to a major earthquake compared to those in thrust or normal fault zones of comparable material properties.

Rigorously speaking, the linearized perturbation theory is correct only to the first-order accuracy in the crack front deviation from a straight line. Hence the first-order perturbation analysis applies to asperities only slightly tougher than their surrounding regions. For moderately tough asperities, while it lies beyond the scope of our linearized analysis, we expect that the more deeply penetrating mode II crack front segments will more readily tend to coalesce unstably with one another, so that the crack front advances and leaves unbroken asperities behind, whereas the mode III crack will require a significantly higher asperity toughness to do so. For mode I cracks penetrating second phase inclusions the transition from breaking through to surrounding particles has been studied by *Fares* [1989] and is found to occur at a toughness ratio of approximately 3.5 for a row of circular obstacles with two diameter center-to-center spacing; on the basis of the linearized perturbation analysis for all three modes, we tentatively expect a lower ratio at transition in mode II and higher in mode III.

The second major result reported in the paper is concerned with whether a straight mode III crack front in the lithosphere along a strike-slip fault will remain in the straight configuration as the slipping crack penetrates upward to cause a major earthquake. By examining the short- and long-wavelength perturbation results, we have shown that a critical wavelength λ_{cr} of the order of the lithosphere thickness H exists above which the stress intensity factor is enhanced rather than diminished at the most advanced portions of the crack front. A full three-dimensional finite element calculation is then performed to determine the exact value of λ_{cr}/H at different crack depths. If the resistance to crack growth is essentially uniform over the fault plane, then the straight crack front is configurationally unstable when $\lambda > \lambda_{cr}$, although significant gradients of fracture resistance can completely stabilize the straight front, or stabilize it to longer wavelengths (see the appendix).

A somewhat related configurational stability problem for rupture of a single circular asperity has been previously considered by *Gao* [1989]. In that case it was found that the circular shape is configurationally stable as long as rigid rotations are fully suppressed at remote field. Thus circular asperities are expected to remain in circular shape during quasi-static crack growth. Interestingly, this is consistent with the dynamic analysis of *Das and Kostrov* [1983] on breaking of a single asperity. They found that the rupture front undergoes a "double pincer" movement starting from the initiation point, indicating that an initially circular asperity tends to retain its circular shape during rupture.

The analysis on configurational stability of fault zones is also motivated by the observation that fault zones, particularly long ones, often do not rupture along their entire length during a single earthquake. This phenomenon has been generally referred to as fault segmentation in the earthquake research community. Increasingly, geological and seismological studies [e.g., *Schwartz and Coppersmith*, 1984; *Schwartz and Sibson*, 1988] indicate that the location of an earthquake rupture is not random, that there exist recognizable physical properties of fault zones which control the nucleation point and lateral extent of rupture and divide a fault into segments, that ruptures with the same characteristics often repeat in the same location, and that independent rupture segments can persist through several seismic cycles.

Although it is natural to attribute fault segmentation to complex structural or geometrical features of fault zones, some aspects may follow from the intrinsic mechanics of faulting to the extent that they would be maintained even if all complexity in the Earth's structure were eliminated. *Horowitz and Ruina* [1989] have demonstrated that complex seismic slip patterns can in special near-neutral stability cases be generated even with no complexity in fault geometry or heterogeneity in material properties. Interestingly, our analysis shows that a spatially homogeneous strike-slip fault zone with completely uniform stressing and material properties is intrinsically unstable at sufficiently long wavelengths. Following this line of investigation, more elaborate crustal earthquake models should be developed, for example, by incorporating in our type of three-dimensional analysis the model of *Tse and Rice* [1986] in which the slip and stress distributions on the fault surface are required to satisfy laboratory-constrained rate- and state-dependent friction laws with properties that vary with temperature and thus with depth. The limited realization of such modeling with frictional properties that are uniform along strike at each depth hints that uniform fault models are inadequate to explain spatiotemporally complex slip. This is at variance with conclusions from inherently discrete models [*Bak and Tang*, 1989; *Carlson and Langer*, 1989; *Ito and Matsuzaki*, 1990], and the issue remains to be resolved.

APPENDIX: EFFECT OF A VERTICAL GRADIENT OF FRACTURE RESISTANCE

Since temperature, normal stress, and pore pressure within a fault zone vary with the vertical coordinate x, we assume here that the fracture toughness $K_c = K_c(x, z)$ varies significantly with x. In order to test if small along-strike perturbations in toughness will cause much larger deviations of the crack front from a straight line, which would signal configurational instability, we assume that $K_c(x, z)$ is nearly independent of z. That slight z dependence can be represented by a Fourier superposition, with coefficients dependent on x. Since we will linearize in the amplitude of any nonuniformities in the z direction, it suffices to consider a single Fourier component, for example,

$$K_c(x, z) = K_{c1}(x)\left[1 - \varepsilon(x) \cos \frac{2\pi z}{\lambda}\right] \tag{A1}$$

where $|\varepsilon| \ll 1$, and to superpose results later.

The crack shape taken in response to that mode of nonuniformity along strike will be of the form $a(z) = a_0 + A \cos(2\pi z/\lambda)$, at least within the linearization, where we assume $|A| \ll a_0$, $|A| \ll H - a_0$. To obtain σ and A, the local $K(z)$ of equation (23) is set equal to $K_c(a(z), z)$ so that, using equation (27) and appropriate linearizations, the fracture criterion $K = K_c$ is

$$\sigma[2H \tan(\pi a_0/2H)]^{1/2}\left\{1 + \left[\frac{\pi}{2H \sin(\pi a_0/H)} - \frac{C(a_0, \lambda)}{\lambda}\right] A \cos(2\pi z/\lambda)\right\} = K_{c1}(a_0) + \left[A \frac{dK_{c1}}{da_0} - \varepsilon(a_0)K_{c1}(a_0)\right] \cos(2\pi z/\lambda) \tag{A2}$$

This criterion will be met if

$$\sigma = K_{c1}(a_0)/[2H \tan(\pi a_0/2H)]^{1/2} \tag{A3}$$

which describes the stress to sustain upward growth of a slip crack with straight front, and

$$A = \varepsilon(a_0)/Q(a_0, \lambda) \tag{A4}$$

where

$$Q(a_0, \lambda) = \frac{dK_{c1}(a_0)/da_0}{K_{c1}(a_0)} + \frac{C(a_0, \lambda)}{\lambda} - \frac{\pi}{2H \sin(\pi a_0/H)} \tag{A5}$$

Since $C(a, \lambda) > 0$, $Q(a, \lambda) > 0$ for sufficiently small λ, and the crack profile then undulates in phase with the reduction of toughness. However, if there exists a sufficiently large wavelength λ such that $Q(a_0, \lambda) = 0$, the straight crack profile is configurationally unstable to perturbations of that wavelength. When $dK_{c1}(a_0)/da_0 = 0$, the critical λ defined by $Q(a_0, \lambda) = 0$ is the same λ_{cr} discussed in connection with Figure 5, confirming our earlier results for configurational stability for crack growth over a fault zone of essentially uniform toughness.

Since we lack direct constraints on $dK_{c1}(a)/da$, we proceed as follows. The straight-crack-front fracture criterion of equation (A3) gives $\sigma = \sigma(a_0)$ and, when differentiated, shows that

$$\frac{d\sigma(a_0)/da_0}{\sigma(a_0)} = \frac{dK_{c1}(a_0)/da_0}{K_{c1}(a_0)} - \frac{\pi}{2H \sin(\pi a_0/H)} \tag{A6}$$

Thus, for example, the assertion that $d\sigma/da_0 > 0$ shows that dK_{c1}/da_0 must exceed a certain positive lower bound. We can use the last expression to rewrite the denominator Q of the perturbation (A4) and (A5) as

$$Q(a_0, \lambda) = \frac{d\sigma(a_0)/da_0}{\sigma(a_0)} + \frac{C(a_0, \lambda)}{\lambda} \tag{A7}$$

This shows that as long as the straight-crack-front configuration grows upward in the lithosphere under increasing tectonic stress σ, $Q > 0$ for all λ. Thus the vertical gradient of K_{c1} stabilizes the straight configuration against small amplitude perturbations of all wavelengths.

The condition $d\sigma/da_0 > 0$ may be too restrictive for realistic representations of tectonic loading. Rather than develop a realistic loading model, such as loading by shear flow in an underlying upper mantle region below a loosely coupled crustal plate [e.g., *Li and Rice*, 1987], we adopt a simpler scenario here. Let us isolate a width W of the plate, extending from $y = -W/2$ to $y = W/2$ in the horizontal direction perpendicular to the strike and regard the relative horizontal displacement Δ in the strike slipping direction as a given, nondecreasing, variable. Then using $k = k(a_0)$ of equation (10) and assuming that W is comparable to or larger than H,

$$\Delta(a_0) = W\sigma(a_0)/\mu + \sigma(a_0)/k(a_0) \tag{A8}$$

where the last term represents the additional compliance of the part-cracked fault zone. Thus one finds

$$\frac{d\Delta(a_0)/da_0}{\Delta(a_0)} = \frac{d\sigma(a_0)/da_0}{\sigma(a_0)} + \frac{2\tan(\pi a_0/2H)}{W + (4H/\pi)\ln[1/\cos(\pi a_0/2H)]}$$
$$= \frac{dK_{c1}(a_0)/da_0}{K_{c1}(a_0)} - \frac{\pi}{2H\sin(\pi a_0/H)} + \frac{2\tan(\pi a_0/2H)}{W + (4H/\pi)\ln[1/\cos(\pi a_0/2H)]} \quad \text{(A9)}$$

and we may rewrite Q as

$$Q(a_0, \lambda) = \frac{d\Delta(a_0)/da_0}{\Delta(a_0)} + \frac{C(a_0, \lambda)}{\lambda} - \frac{2\tan(\pi a_0/2H)}{W + (4H/\pi)\ln[1/\cos(\pi a_0/2H)]} \quad \text{(A10)}$$

At the onset of dynamically unstable crack growth the crack has reached a length a_0 at which $dK_{c1}(a_0)/da_0$ is sufficiently small that $da_0/d\Delta \to \infty$, which is equivalent to $d\Delta(a_0)/da_0 \to 0$. Whenever the cracked fault zone is sufficiently close to this condition, so that the sum of the first and third terms in Q is negative, the straight front configuration will be unstable to sufficiently long wavelengths λ, since there will exist a λ at which $Q(a_0, \lambda) = 0$. As an example, suppose that the system is sufficiently close to dynamical instability that $d\Delta(a_0)/da_0$ is negligibly small and that this happens, for example, at $a_0 = H/2$; there results $\lambda \simeq 3W + 1.3H$ at configurational instability (observe from Figure 7 that when $a_0/H = 0.5$, C is nearly 6 for a wide range of λ/H). If W is taken to be of the same order as H, the above wavelength is comparable to $\lambda_{cr} \simeq 4H$ (from Figure 5b) for the case when the fracture toughness is essentially uniform. If dK_{c1}/da_0 were not close to that for dynamic instability, the result $\lambda \simeq 3W + 1.3\,H$ would be a lower bound to the λ at configurational instability, and a significant increase of dK_{c1}/da_0 might preclude configurational instability at any wavelength.

Acknowledgments. H.G. and J.L. acknowledge support by the National Science Foundation under grant MSS-9008521, and J.R.R. acknowledges support by the U.S. Geological Survey under grants 14-08-0001-G1367 and 14-08-0001-G1788. We thank G. M. Mavko and P. Segall of the Department of Geophysics at Stanford University, J. Boatwright and J. Andrews of U.S. Geological Survey, and another anonymous reviewer for helpful comments and discussions on the paper.

REFERENCES

Bak, P., and C. Tang, Earthquakes as self-organized critical phenomena, *J. Geophys. Res.*, *94*, 15,635–15,637, 1989.
Bower, A. F., and M. Ortiz, Solution of three-dimensional crack problems by a finite perturbation method, *J. Mech. Phys. Solids*, *38*, 443–480, 1990.
Carlson, J. M., and J. S. Langer, Properties of earthquakes generated by fault dynamics, *Phys. Rev. Lett.*, *62*, 2632–2635, 1989.
Das, S., and B. V. Kostrov, Breaking of a single asperity: Rupture process and seismic radiation, *J. Geophys. Res.*, *88*, 4277–4288, 1983.
Delale, F., and F. Erdogan, Application of the line-spring model to a cylindrical shell containing a circumferential or axial part-through crack, *J. Appl. Mech.*, *49*, 97–102, 1982.
Fares, N., Crack fronts trapped by arrays of obstacles: Numerical solutions based on surface integral representation, *J. Appl. Mech.*, *56*, 837–843, 1989.
Gao, H., Nearly circular shear mode cracks, *Int. J. Solids Struct.*, *24*, 177–193, 1988.
Gao, H., Linear perturbation analysis of a single asperity, *J. Geophys. Res.*, *94*, 10,259–10,265, 1989.
Gao, H., and J. R. Rice, Shear stress intensity factors for a planar crack with slightly curved front, *J. Appl. Mech.*, *53*, 774–778, 1986.
Gao, H., and J. R. Rice, A first order perturbation analysis on crack trapping by arrays of obstacles, *J. Appl. Mech.*, *56*, 828–836, 1989.
Horowitz, F. G., and A. Ruina, Slip patterns in a spatially homogeneous fault model, *J. Geophys. Res.*, *94*, 10,279–10,298, 1989.
Ito, K., and M. Matsuzaki, Earthquakes as self-organized critical phenomena, *J. Geophys. Res.*, *95*, 6853–6860, 1990.
Krstic, V. D., On the fracture of brittle-matrix/ductile-particle composites, *Philos. Mag. A*, *48*, 695–708, 1983.
Lay, T., and H. Kanamori, An asperity model of great earthquake sequences, in *Earthquake Prediction: An International Review*, *Maurice Ewing Ser.*, vol. 4, edited by D. W. Simpson and P. G. Richards, pp. 579–592, AGU, Washington, D. C., 1981.
Lay, T., H. Kanamori, and L. Ruff, The asperity model and the nature of large subduction zone earthquake occurrence, *Earthquake Predict. Res.*, *1*, 3–71, 1982.
Li, V. C., and J. R. Rice, Preseismic rupture progression and great earthquake instabilities at plate boundaries, *J. Geophys. Res.*, *88*, 4231–4246, 1983.
Li, V. C., and J. R. Rice, Crustal deformation in great California earthquake cycles, *J. Geophys. Res.*, *92*, 11,533–11,551, 1987.
Lynn, P. P., and A. R. Ingraffea, Transition elements to be used with quarter-point crack-tip elements, *Int. J. Numer. Methods Eng.*, *12*, 1031–1036, 1978.
Madariaga, R., On the relation between seismic moment and drop in the presence of stress and strength heterogeneity, *J. Geophys. Res.*, *84*, 2243–2250, 1979.
McGarr, A., Analysis of peak ground motion in terms of a model of inhomogeneous faulting, *J. Geophys. Res.*, *86*, 3901–3912, 1981.
Mitchell, T. E., and R. L. Smialek, The stress to operate a Frank-Read source in *Work Hardening*, edited by J. P. Hirth and J. Weertman, pp. 365–382, Gordon and Breach, New York, 1968.
Nabarro, F. R. N., *Theory of Crystal Dislocations*, Oxford University Press, New York, 1967.
Parks, D. M., Virtual crack extension: A general finite element technique for *J*-integral evaluation, in *Numerical Methods in Fracture Mechanics*, edited by A. R. Luxmoore and D. R. J. Owen, pp. 464–478, Pineridge Press, Swansea, England, 1978.
Parks, D. M., R. R. Lockett, and J. R. Brockenbrough, Stress intensity factors for surface cracked plates and cylindrical shells using line spring finite elements, in *Advances in Aerospace Structures and Materials*, vol. AD-01, edited by S. S. Wang and W. J. Renton, pp. 279–285, American Society of Mechanical Engineering, New York, 1981.
Prescott, W. H., and A. Nur, The accommodation of relative motion at depth on the San Andreas fault system in California, *J. Geophys. Res.*, *86*, 999–1004, 1981.
Rice, J. R., The mechanics of earthquake rupture, in *Physics of Earth's Interior*, edited by A. M. Dziewonsky and E. Boschi, pp. 555–649, North-Holland, New York, 1980.
Rice, J. R., First order variations in elastic fields due to variation in location of a planar crack front, *J. Appl. Mech.*, *52*, 571–579, 1985.
Rice, J. R., Weight function theory for three-dimensional crack analysis, in Fracture Mechanics: Perspectives and Directions (Twentieth Symposium), edited by R. P. Wei and R. P. Gangloff, *ASTM Spec. Tech. Publ.*, *1020*, 29–57, 1989.
Rice, J. R., Spatio-temporally complex fault slip: 3D simulations with rate- and state-dependent friction on a fault surface between elastically deformable continua (abstract), *Eos Trans. AGU*, *72*(17), suppl., 278, 1991.
Rice, J. R., and N. Levy, The part through surface crack in an elastic plate, *J. Appl. Mech.*, *39*, 185–194, 1972.

Savage, J. C., and R. O. Burford, Geodetic determination of relative plate motion in central California, *J. Geophys. Res.*, *78*, 832–845, 1973.
Scholz, C. H., *The Mechanics of Earthquakes and Faulting*, Cambridge University Press, New York, 1990.
Schwartz, D. P., and K. J. Coppersmith, Fault behavior and characteristic earthquakes: Examples from the Wasatch and San Andreas fault zones, *J. Geophys. Res.*, *89*, 5681–5698, 1984.
Schwartz, D. P., and R. H. Sibson, Proceedings of Workshop XLV on Fault Segmentation and Controls of Rupture Initiation and Termination, *Rep. OFP 89-315*, U.S. Geol. Surv., Menlo Park, Calif., 1988.
Stuart, W. D., Strain softening instability model for the San Fernando earthquake, *Science*, *203*, 907–910, 1979.
Stuart, W. D., Forecast model for great earthquakes at the Nankai Trough subduction zone, *Pure Appl. Geophys.*, *126*, 619–641, 1988.
Stuart, W. D., and G. M. Mavko, Earthquake instability on a strike-slip fault, *J. Geophys. Res.*, *84*, 2153–2160, 1979.
Tada, H., P. C. Paris, and G. R. Irwin, *The Stress Analysis of Cracks Handbook*, Del Research Corporation, Hellertown, Pa., 1985.
Tse, S. T., and J. R. Rice, Crustal earthquake instability in relation to the depth variation of frictional slip properties, *J. Geophys. Res.*, *91*, 9452–9472, 1986.
Tse, S. T., R. Dmowska, and J. R. Rice, Stressing of locked patches along a creeping fault, *Bull. Seismol. Soc. Am.*, *75*, 709–736, 1985.
Turcotte, D. L., and D. A. Spence, An analysis of strain accumulation on a strike-slip fault, *J. Geophys. Res.*, *79*, 4407–4412, 1974.

H. Gao and J. Lee, Division of Applied Mechanics, Durand 267, Stanford University, Stanford, CA 94305.
J. R. Rice, Division of Applied Sciences, Harvard University, Cambridge, MA 02138.

(Received November 13, 1990;
revised August 9, 1991;
accepted August 30, 1991.)